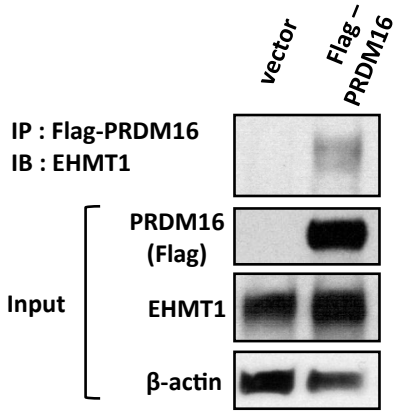

Supplementary Figure 1. PRDM16 interacts with endogenous EHMT1 in brown adipocytes.

Immunoprecipitation of PRDM16 complex by flag antibody (M2) followed by Western blot analysis to detect endogenous EHMT1 protein in brown adipocytes. Inputs are shown in lower panels.

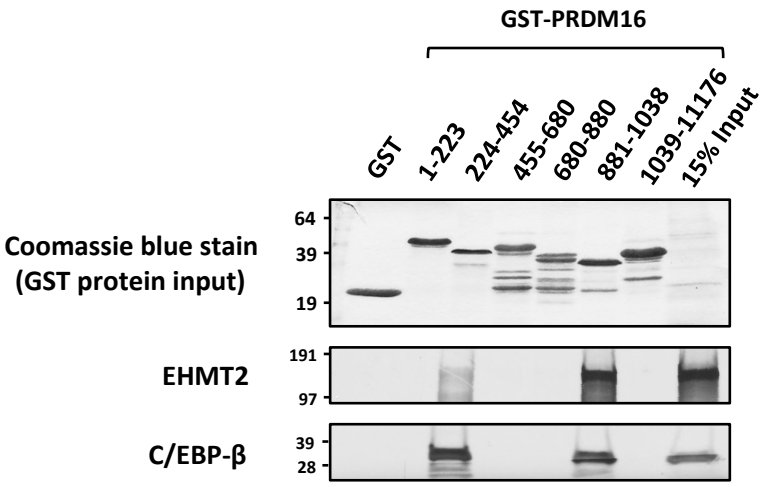

Supplementary Figure 2. Interaction between purified PRDM16 fragments and EHMT2 or C/EBP-β.

In vitro binding assay of ^{35}S-labeled EHMT2 or C/EBP-β and purified GST-fusion fragments of PRDM16 (as indicated). GST-fusion proteins were separated by SDS-PAGE, and stained by Coomassie brilliant blue (top panel). EHMT2 and C/EBP-β proteins were detected by autoradiography.

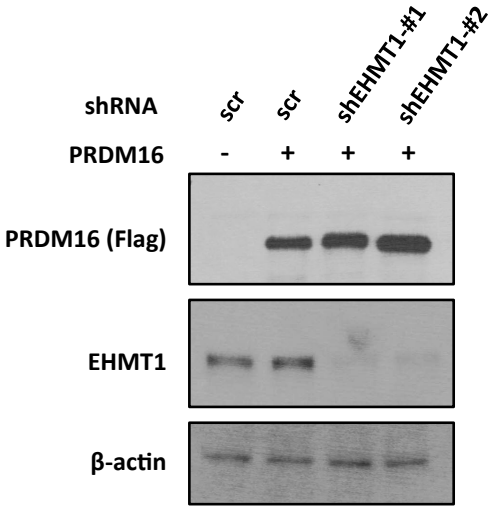

Supplementary Figure 3. Depletion of EHMT1 by two different shRNAs targeted to EHMT1 in brown adipocytes.

Flag tagged PRDM16 was overexpressed in immortalized brown adipocytes by retrovirus. EHMT1 was depleted by retrovirus-mediated shRNAs for a scramble control (scr), shEHMT1-#1, and shEHMT1-#2. Flag tagged PRDM16 and endogenous EHMT1 protein were detected by Western blotting. β-actin protein was shown as a loading control.

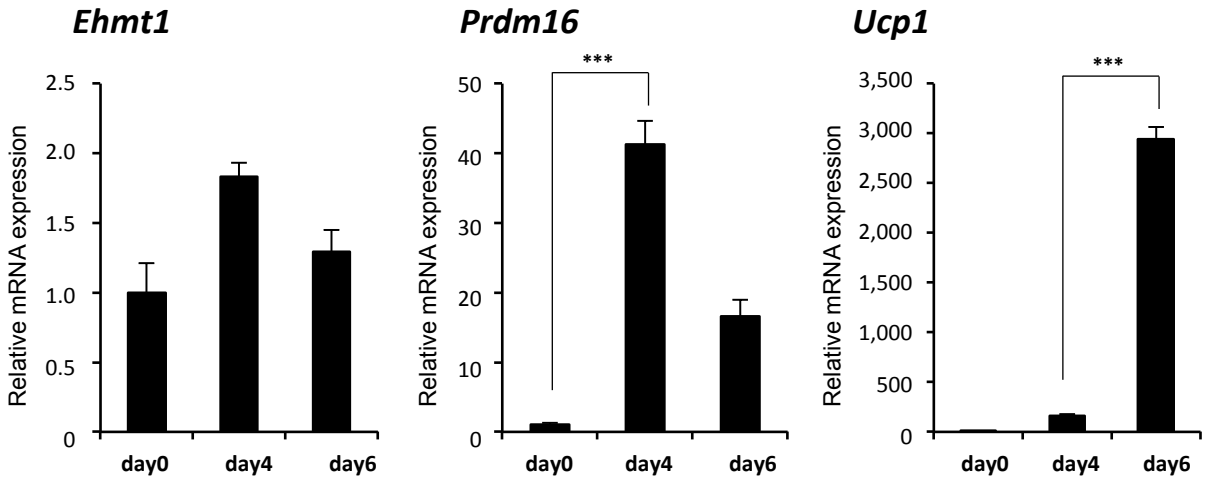

Supplementary Figure 4. Changes in EHMT1 expression during brown adipocyte differentiation.

mRNA levels of *Ehmt1*, *Prdm16* and *Ucp1* were measured during the differentiation of immortalized brown adipocytes by qRT-PCR. n=3; data are presented as mean and s.e.m. *** P <0.001.

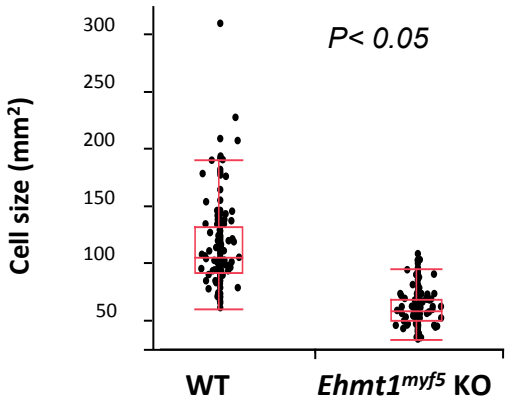

Supplementary Figure 5. Adipocyte cell size of the interscapular BAT from wild-type (WT) and *Ehmt1*^{myf5} KO embryos at P1 stage.

Brown adipocyte size was quantified in the BAT of wild-type (WT) and *Ehmt1*^{myf5} KO embryos at P1 using Image J software. n=145-154.

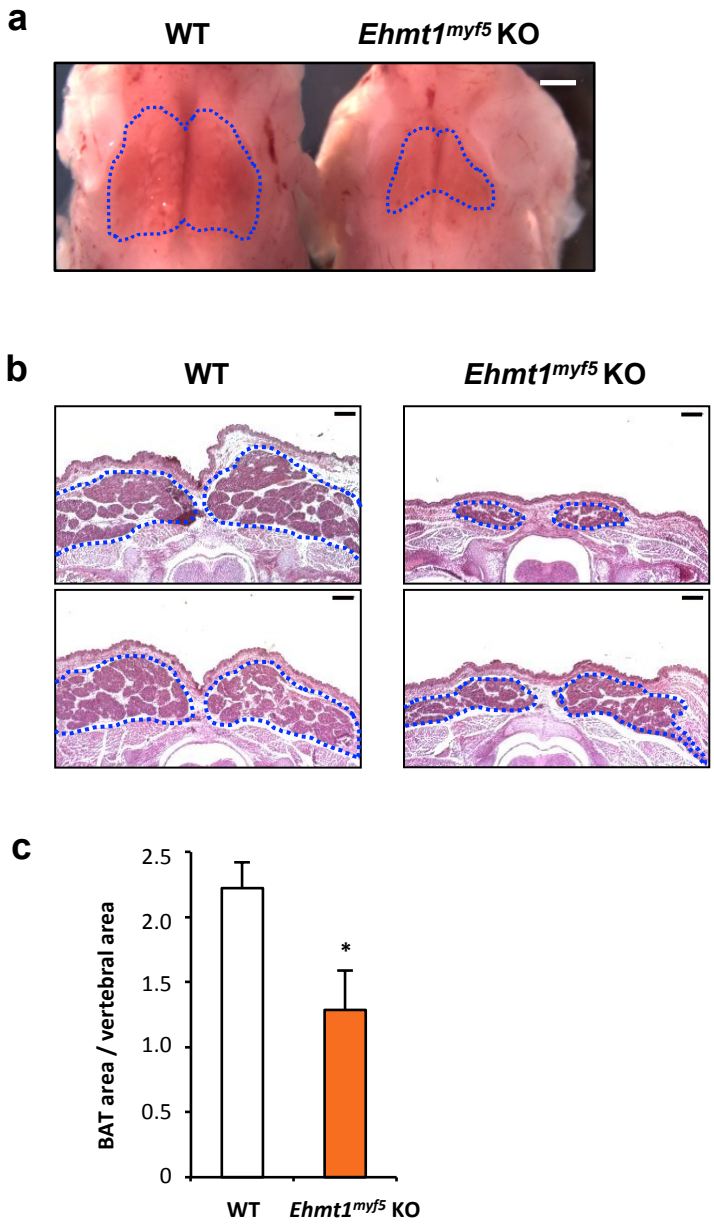

Supplementary Figure 6. Morphological characterization of *Ehmt1*^{myf5} KO embryos at E18.5.

a, Gross pictures of wild-type (WT) and *Ehmt1*^{myf5} KO embryos at E18.5. BAT is highlighted by dashed lines. Scale bar, 1 mm. **b,** Haematoxylin and eosin (H&E) staining of transverse sections of wild-type and *Ehmt1*^{myf5} KO embryos. Sections containing the largest area of BAT were shown. BAT is highlighted by dashed lines. Scale bar, 300 μm. **c,** Quantification of the BAT size of WT and *Ehmt1*^{myf5} KO embryos derived from multiple breeding pairs. The BAT size was normalized by vertebral size. n=4 per genotype. All error bars are s.e.m.; * $P< 0.05$.

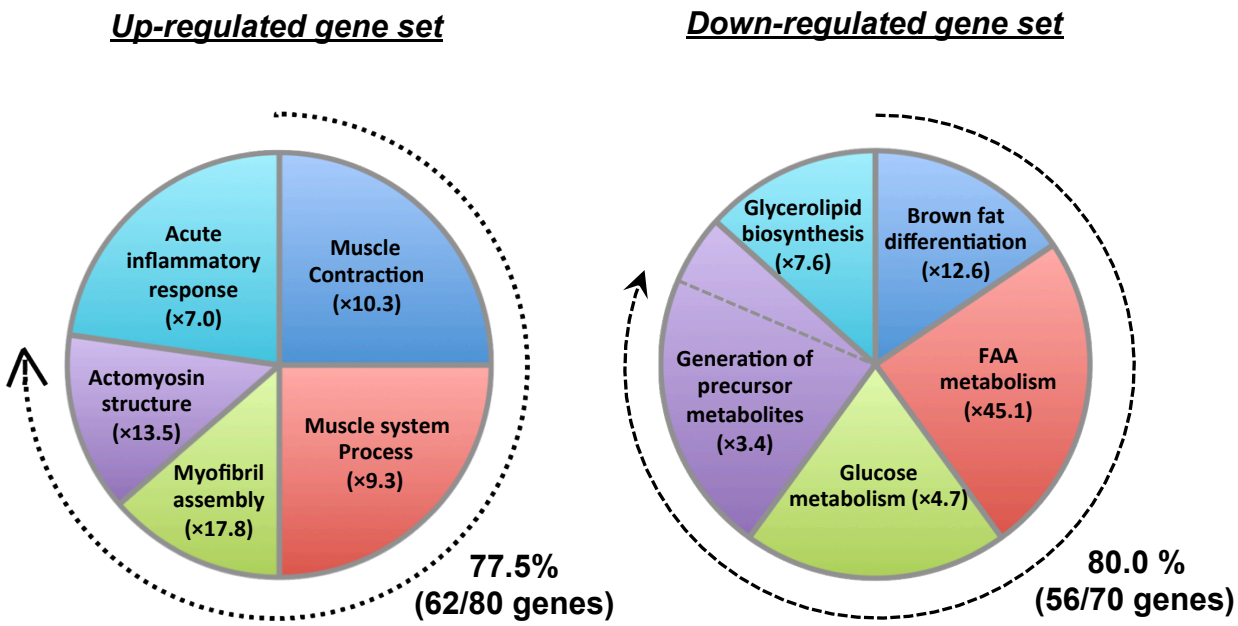

Supplementary Figure 7. EHMT1 controls cell fate determination between skeletal muscle *versus* brown fat.

RNA-sequencing and gene ontology (GO) analyses identified clusters of genes that were coordinately up-regulated (left) or down-regulated (right) in the BAT from *Ehmt1*^{myf5} KO mice as compared to that from wild-type mice. These clusters were annotated to the GO terms as shown in each pie slice. Fold enrichments of the each GO cluster are shown. Area of each pie slice are proportional to the number of genes.

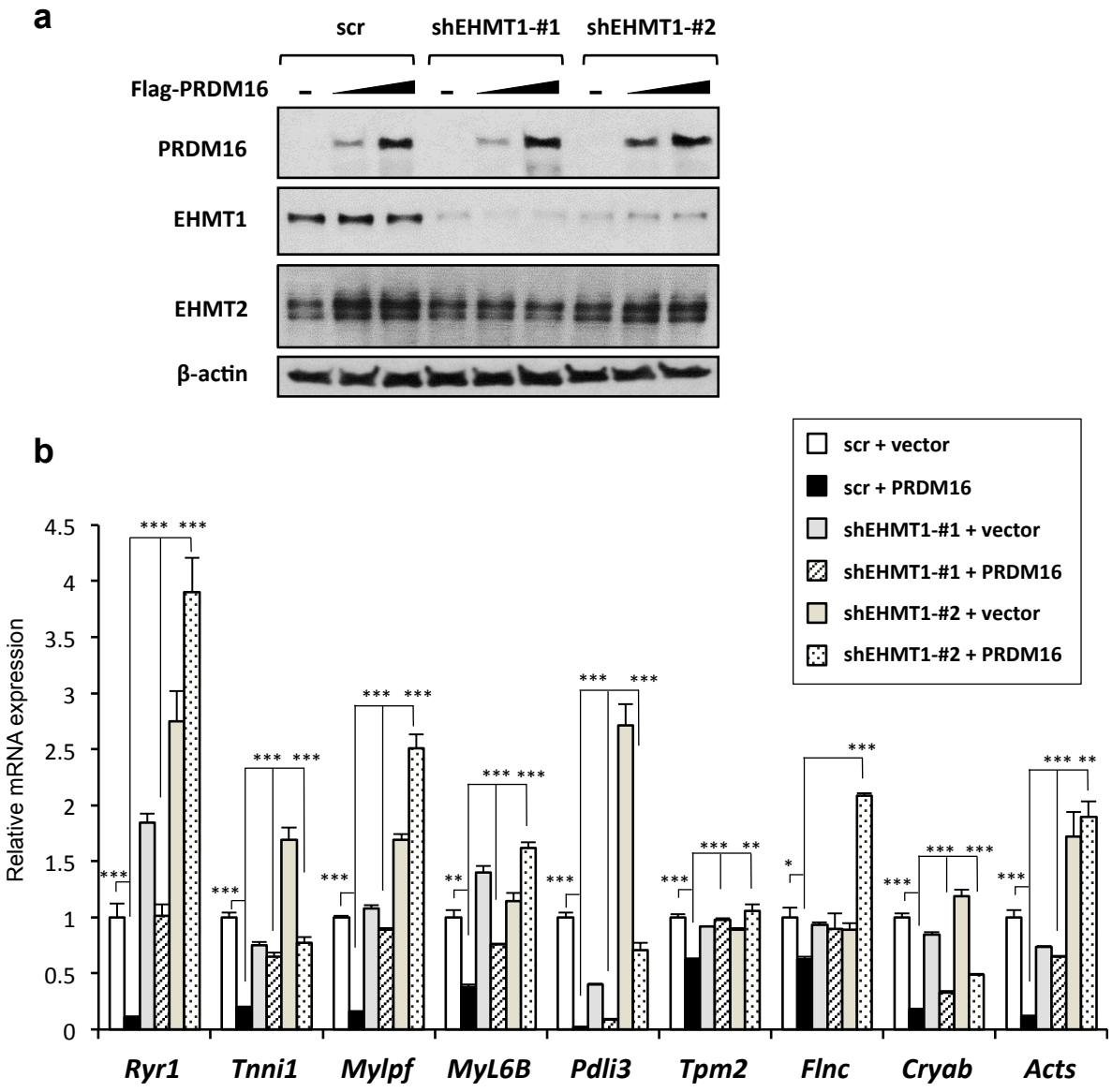

Supplementary Figure 8. EHMT1 is required for PRDM16-mediated repression on muscle-selective genes.

a, C2C12 myoblasts were transduced with scrambled control (scr) or shRNAs targeted to EHMT1 (shEHMT1-#1 and shEHMT1-#2) together with PRDM16 or vector control. Protein levels of PRDM16, EHMT1 and EHMT2 were detected by Western blotting. β-actin protein was shown as a loading control. **b,** mRNA expression of muscle-selective genes (as indicated) was measured by qRT-PCR. n=3; data are presented as mean and s.e.m.; * $P< 0.05$, ** $P <0.01$, *** $P <0.001$.

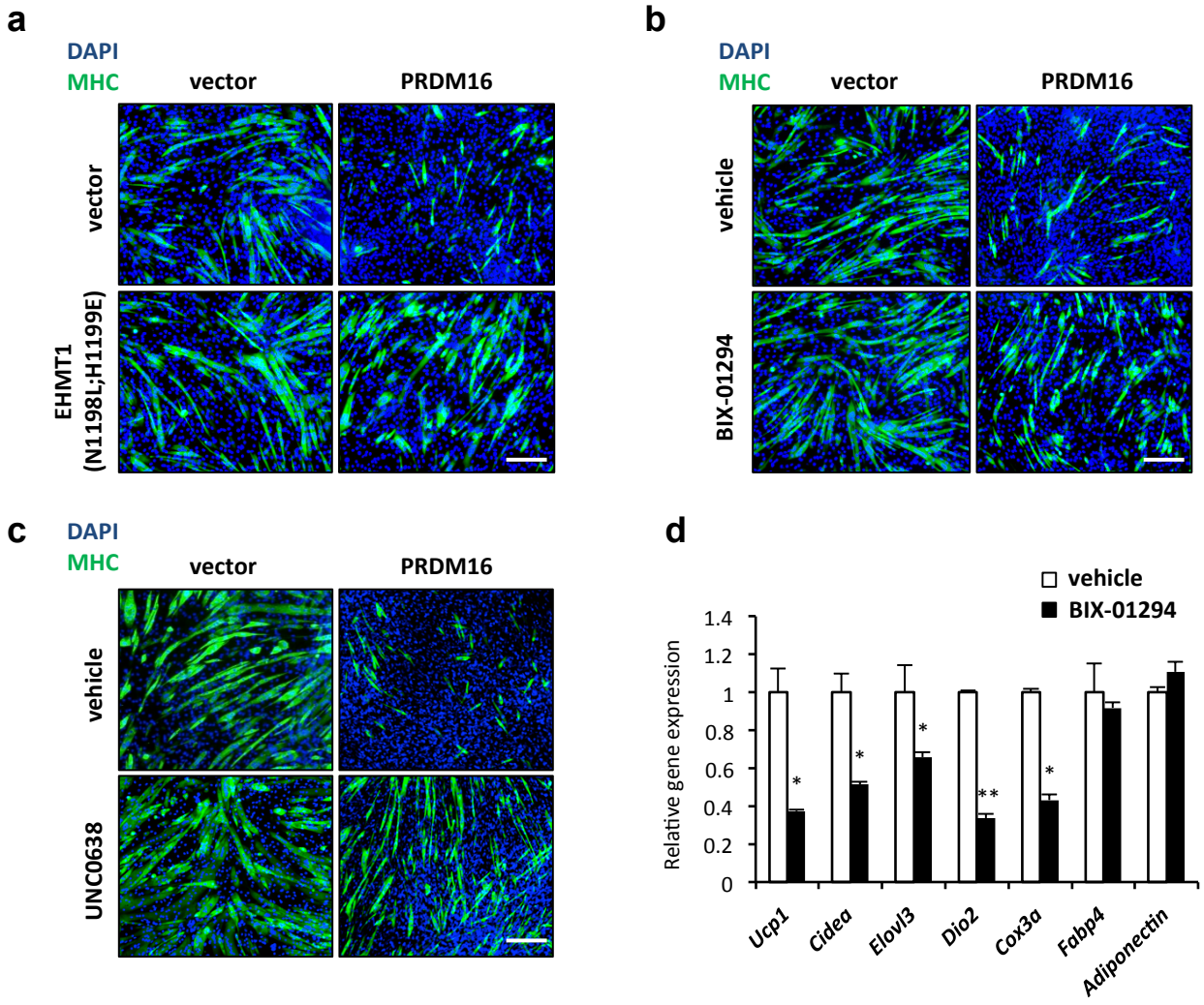

Supplementary Figure 9. Repressive effect of EHMT1 on myogenesis is mediated through its methyltransferase activity.

a, The SET-domain mutant of EHMT1 (p. N1198L;H1199E) or vector was overexpressed in C2C12 myoblasts in the presence or absence of PRDM16. These cells were differentiated under pro-myogenic culture conditions. Differentiated myotubes were visualized by immunocytochemistry for skeletal myosin heavy chain (MHC). Nuclei were stained with DAPI (4′,6-diamidino-2-phenylindole). Scale bar, 200μm. **b-c,** C2C12 myoblasts expressing PRDM16 or vector control were differentiated under pro-myogenic culture conditions in the presence or absence of chemical inhibitors for EHMT1/2, BIX-01294 (b, 2.5 μM) or UNC0638 (c, 1.0 μM). Differentiated myotubes were stained with MHC antibody. Nuclei were counterstained with DAPI. Scale bar, 200μm. **d,** Brown adipocytes were treated with BIX-01294 under pro-adipogenic culture conditions. mRNA levels of BAT-selective genes (as indicated) were measured by qRT-PCR. n=3; data are presented as mean and s.e.m.; * $P< 0.05$, ** $P <0.01$.

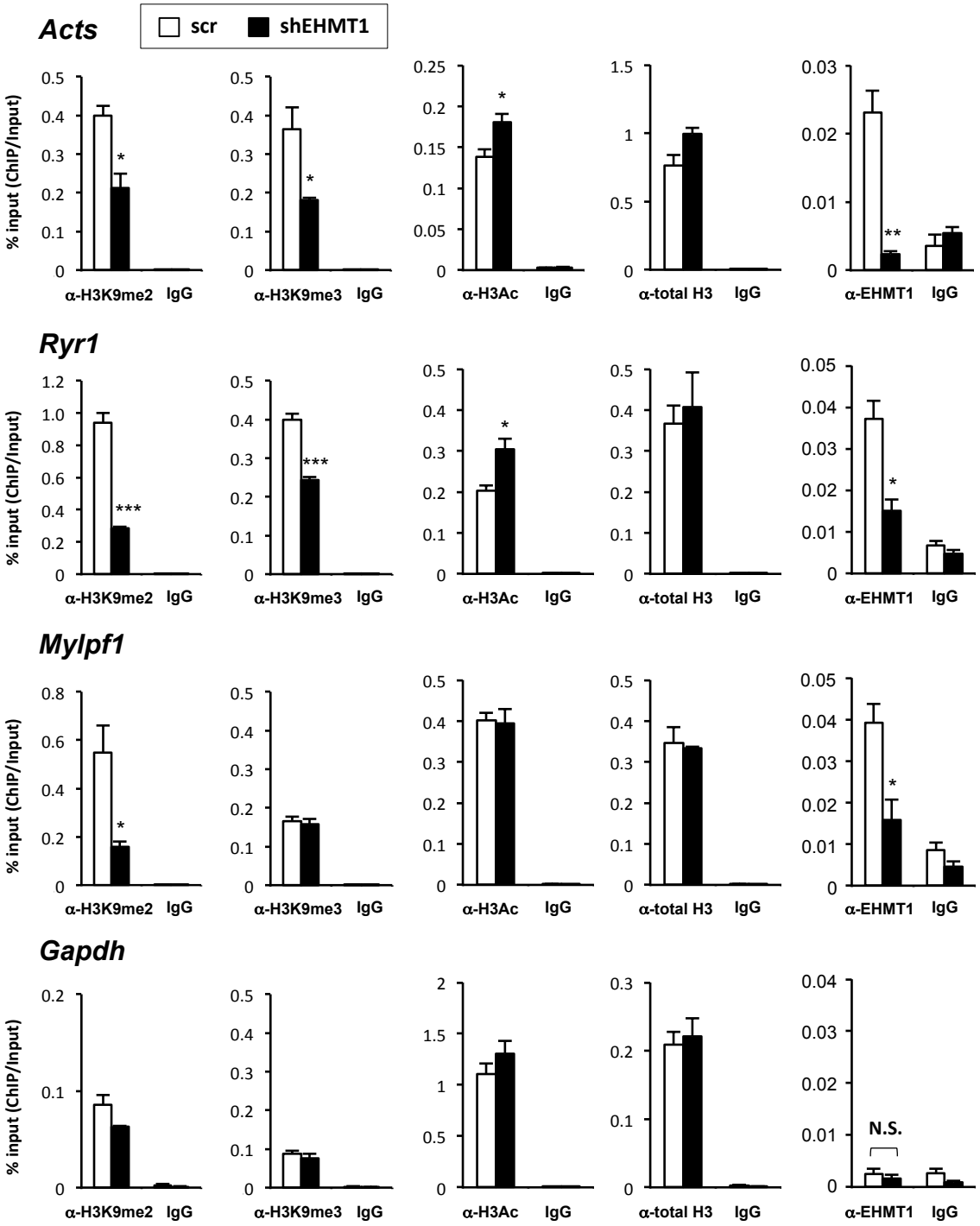

Supplementary Figure 10. EHMT1 controls H3K9 methylation status on the promoter regions of muscle-selective genes.

ChIP assays were performed on the promoters of muscle-selective genes (as indicated) using antibodies against H3K9me2, H3K9me3, H3K9/K14ac, pan-H3, EHMT1, and IgG. White and black columns represent scr control and shEHMT1, respectively. ChIP assays were also performed on the promoter of *Gapdh,* a non-muscle related gene. n=3; data are presented as mean and s.e.m.; * $P< 0.05$, ** $P <0.01$, *** $P <0.001$.

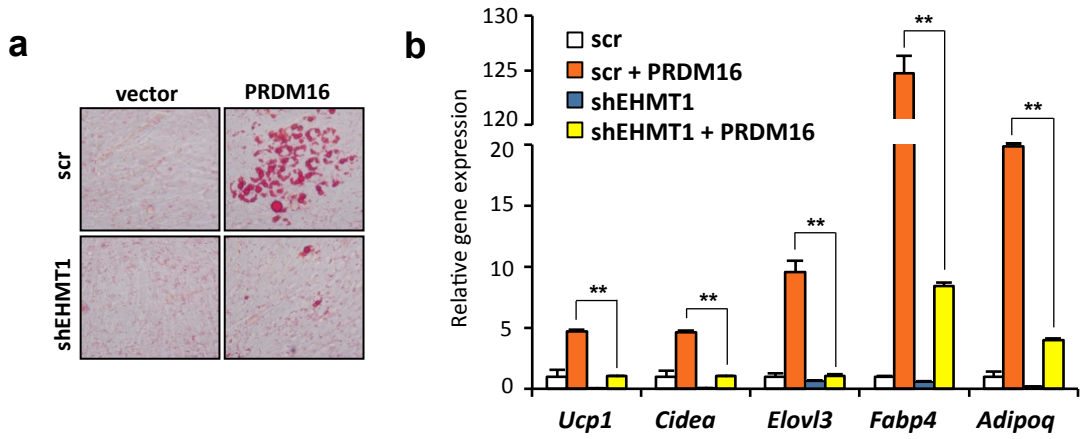

Supplementary Figure 11. Knockdown of EHMT1 blocked the PRDM16-induced brown adipogenesis.

a, Oil-Red-O staining of C2C12 cells expressing indicated constructs. C2C12 myoblasts were transduced with scrambled control (scr) or shRNA targeted to EHMT1 (shEHMT1-#1) together with PRDM16 or vector control, and differentiated under pro-adipogenic culture conditions for 8 days. **b,** mRNA expression of BAT-selective genes and adipogenic marker genes (as indicated) in a. n=3. All error bars are s.e.m.; ** P <0.01.

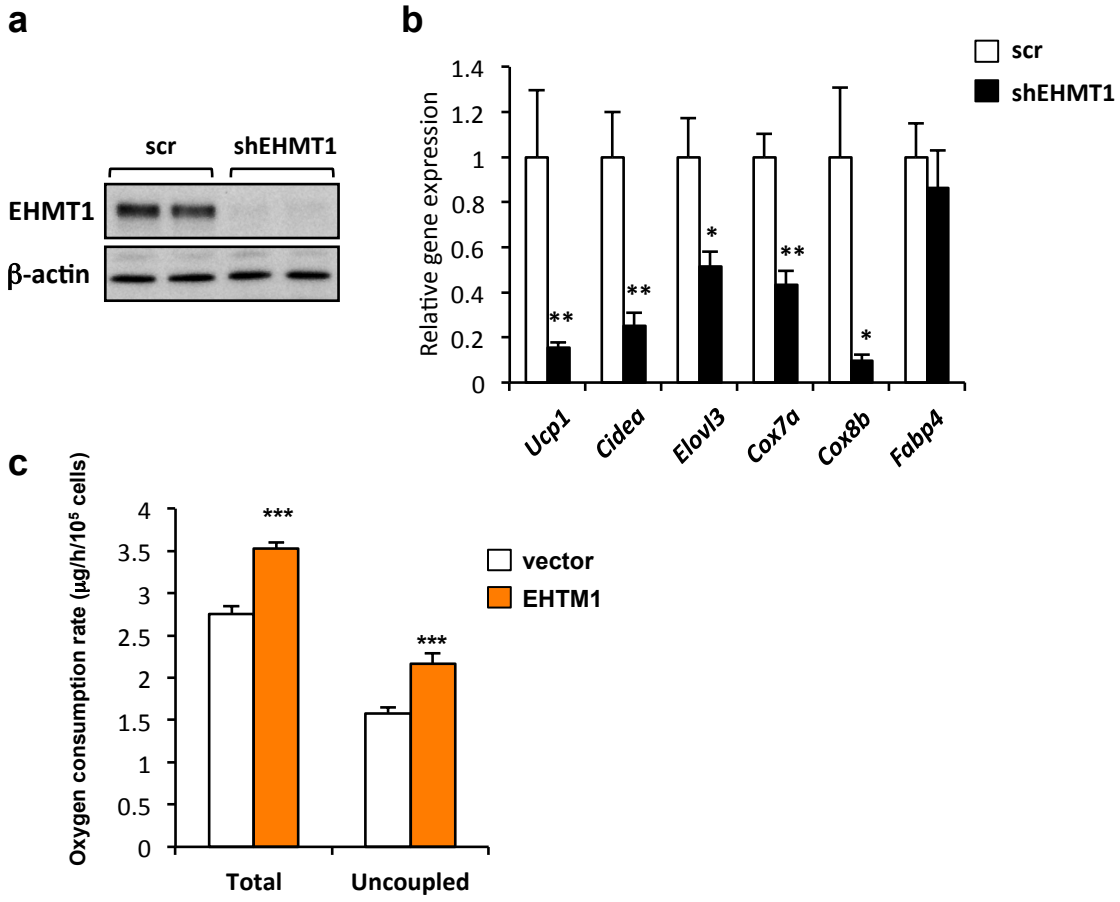

Supplementary Figure 12. EHMT1 controls the BAT-selective thermogenic program in brown adipocytes.

a, EHMT1 was depleted in immortalized brown adipocytes by retrovirus-mediated shRNA knockdown (shEHMT1-#1). Endogenous EHMT1 protein was detected by Western blotting. β-actin protein was shown as a loading control. **b,** mRNA expression of BAT-selective genes (as indicated) was measured in differentiated brown adipocytes by qRT-PCR. n=3. **c,** Total and uncoupled (oligomycin-insensitive) cellular oxygen consumption rate was measured in differentiated brown adipocytes expressing vector or EHMT1. n=6. Data are presented as mean and s.e.m.; * $P< 0.05$, ** $P <0.01$, *** $P<0.001$.

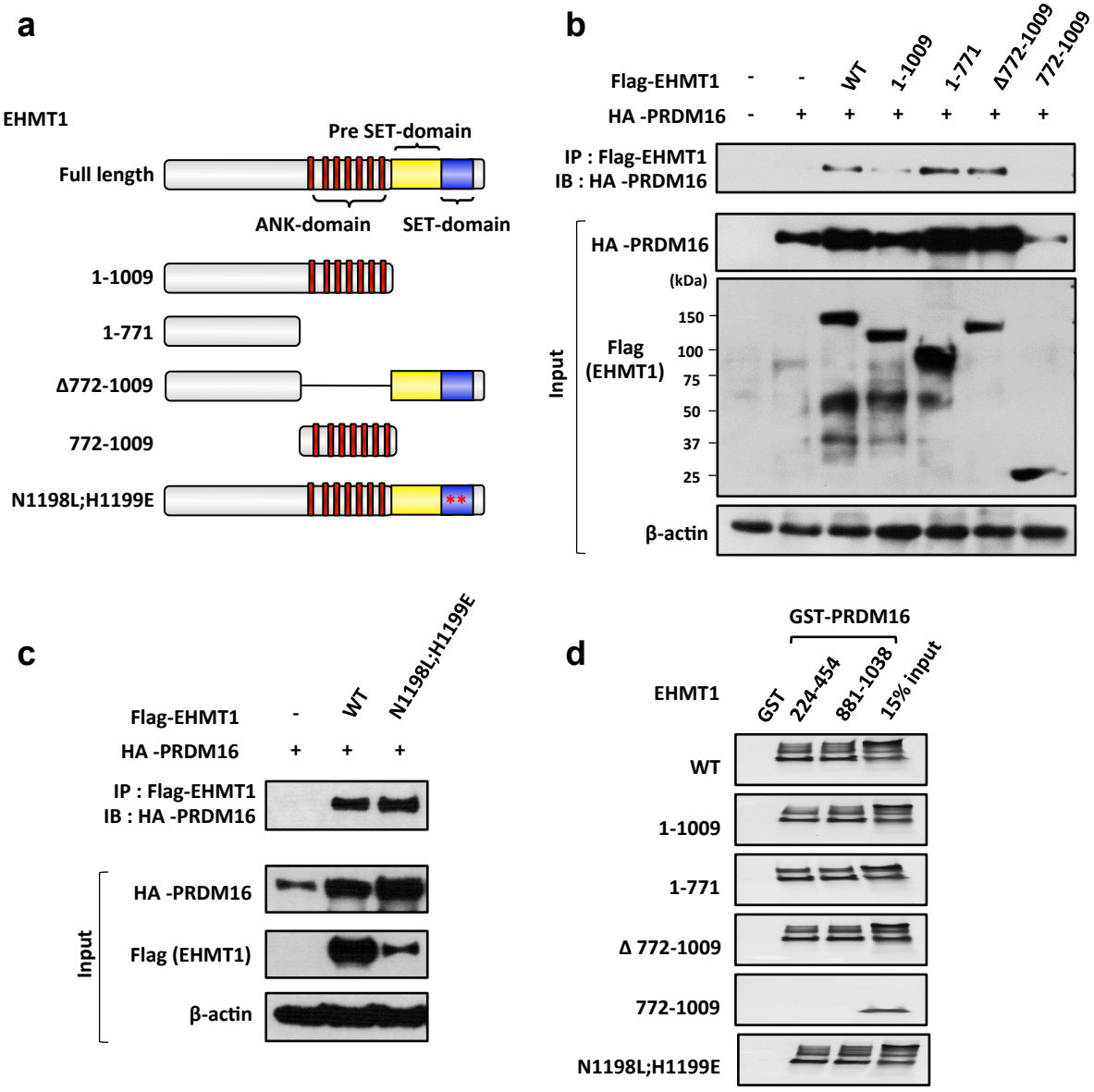

Supplementary Figure 13. Mapping of EHMT1 domains that are required for interaction with PRDM16.

a, Schematic illustration of EHMT1 protein structure. Deletion mutants and a point mutant of EHMT1 are shown. Two mutations in the N1198L;H1199E mutant are indicated by stars. **b-c,** HA-tagged full length PRDM16 was transiently expressed together with wild-type or the mutant forms of EHMT1 (as indicated) in COS7 cells. EHMT1 was immunoprecipitated using flag M2 antibody, separated by SDS-PAGE, and PRDM16 protein was detected by Western blotting. The inputs are shown in bottom panels. **d,** *In vitro* binding assay of ^{35}S-labeled EHMT1 mutants (as indicated) and purified GST-PRDM16 fusion proteins. GST-fusion proteins were separated by SDS-PAGE. EHMT1 proteins were detected by autoradiography.

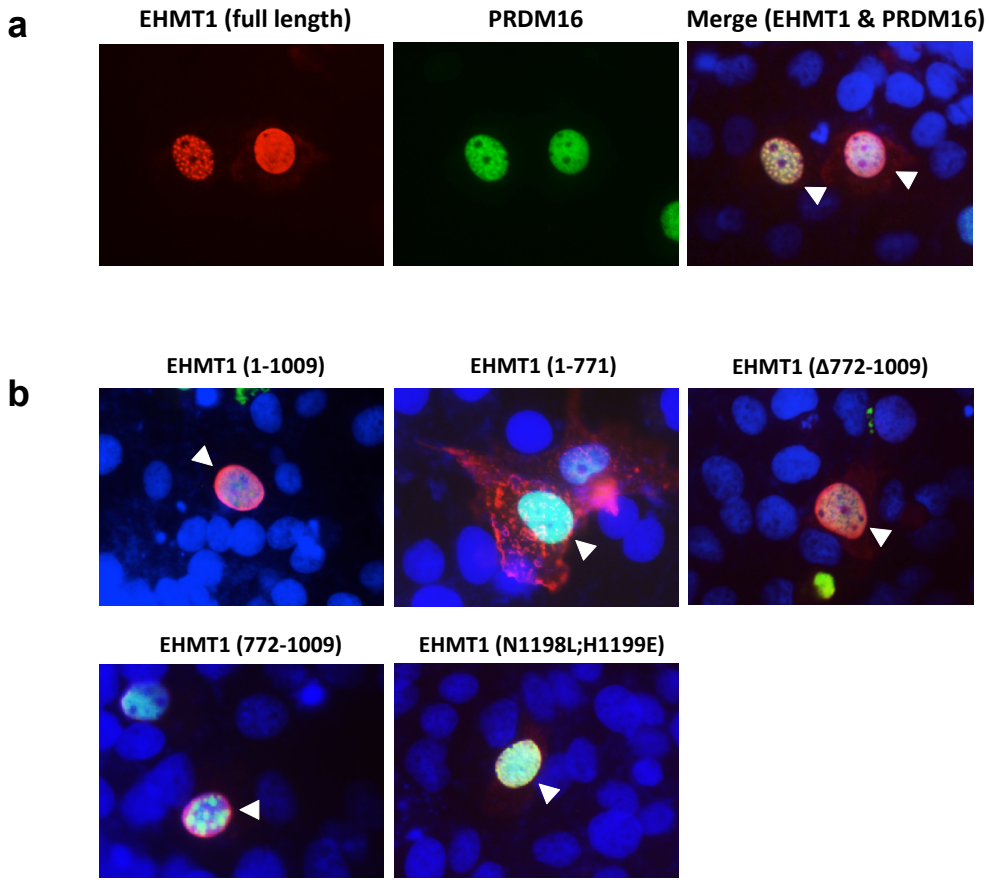

Supplementary Figure 14. Mapping of EHMT1 domains that are required for co-localization with PRDM16.

a, Nuclear localization of full length EHMT1 (red, left) and PRDM16 (green, middle). Flag-tagged EHMT1 and GFP-PRDM16 were transiently expressed in COS7 cells. Flag-EHMT1 was immunostained using M2 flag antibody. Nuclei were stained with DAPI (4′,6-diamidino-2-phenylindole). Merged image (right) shows co-localization of EHMT1 and PRDM16 in nucleus, as indicated by arrow heads. **b,** Flag-tagged deletion mutants and point mutant of EHMT1were transiently expressed together with GFP-PRDM16 in COS7 cells. Co-localization of EHMT1 and PRDM16 were shown by arrow heads. Note that the 1-771 region of EHMT1 was ubiquitously expressed.

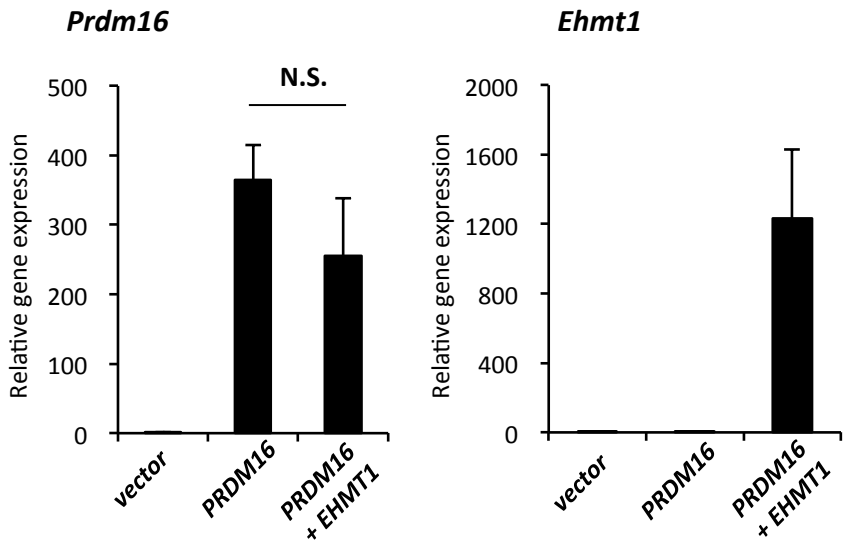

Supplementary Figure 15. Ectopic expression of EHMT1 does not affect mRNA expression of PRDM16 in the protein stability assay.

EHMT1 was transiently expressed together with PRDM16 or vector in COS7 cells. Forty-eight hours after transfection, total RNA was extracted from the cells and treated with DNase I. Subsequently, mRNA expression of ectopically expressed flag-tagged PRDM16 was measured by qRT-PCR. n=3; Data are presented as mean and s.e.m.

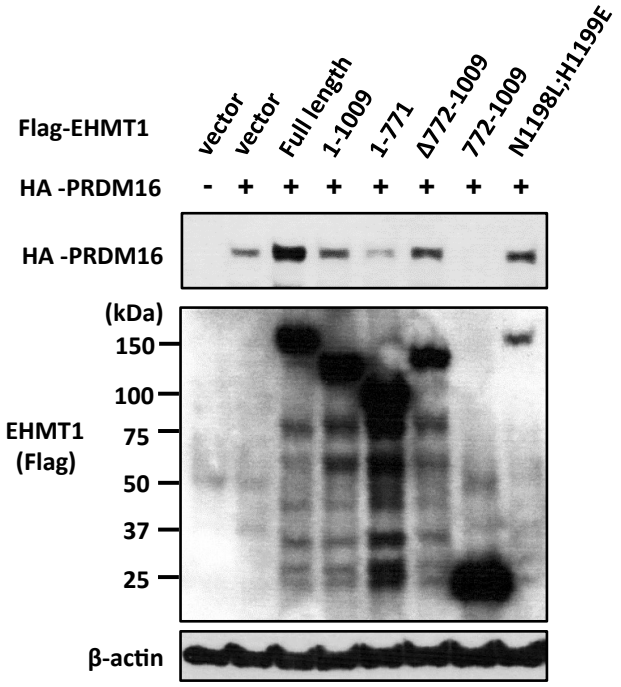

Supplementary Figure 16. EHMT1 induces protein accumulation of PRDM16 through direct interaction.

HA-tagged PRDM16 was transiently expressed together with wild-type or the mutant forms of EHMT1 (as indicated) or vector. Total cell lysates were isolated 48 hours after transfection, and subjected to SDS-PAGE. PRDM16 and EHMT1 were detected by Western blotting using HA or flag antibody. β-actin protein was shown as a loading control.

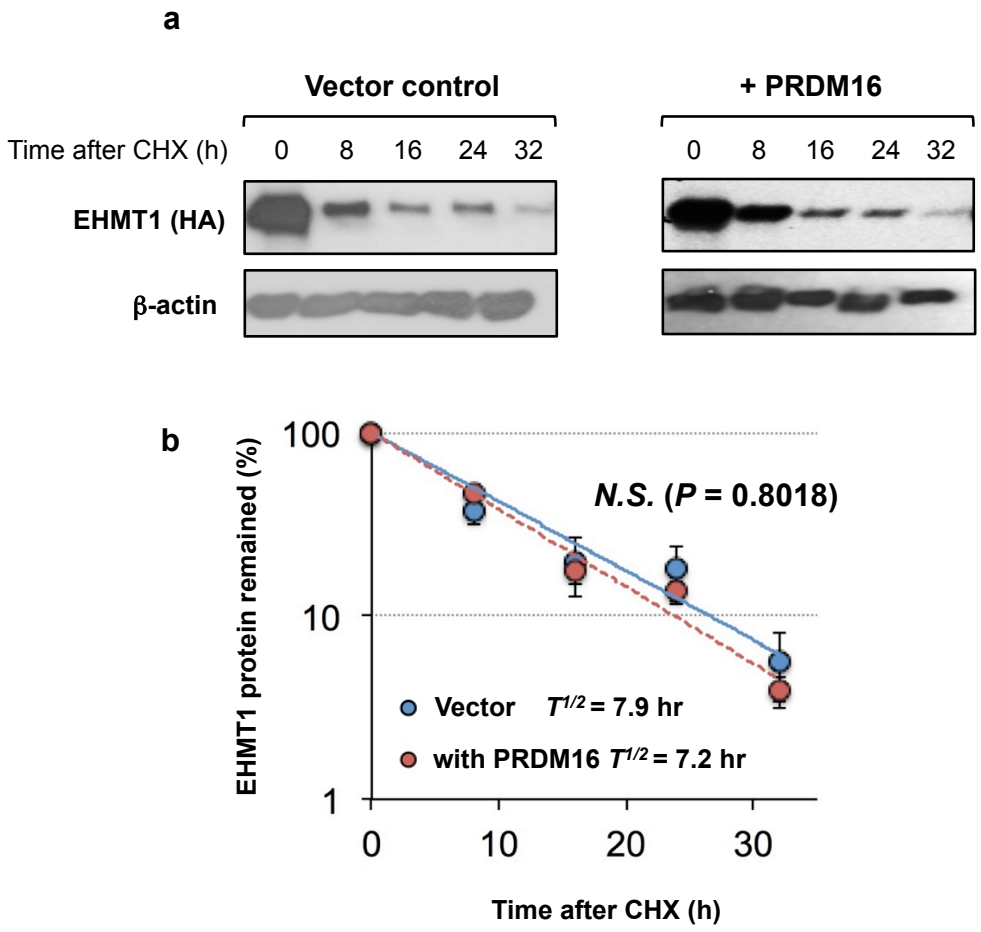

Supplementary Figure 17. EHMT1 protein stability is not affected by PRDM16 expression.

a, EHMT1 protein stability was assessed by cycloheximide (CHX) chase experiments in the presence or absence of PRDM16. COS7 cells were transiently expressed with full length EHMT1 together with PRDM16 or vector control. Cells were treated with CHX for indicated hours and harvested. EHMT1 protein levels were analyzed by Western blotting. β-actin protein was shown as a loading control. **b,** Regression analysis of EHMT1 protein stability in a. Significance between curves was determined by two-way repeated measures ANOVA. *P* value of main effect (vector or PRDM16) was not significant. n=3 per group. Data are presented as mean and s.e.m.

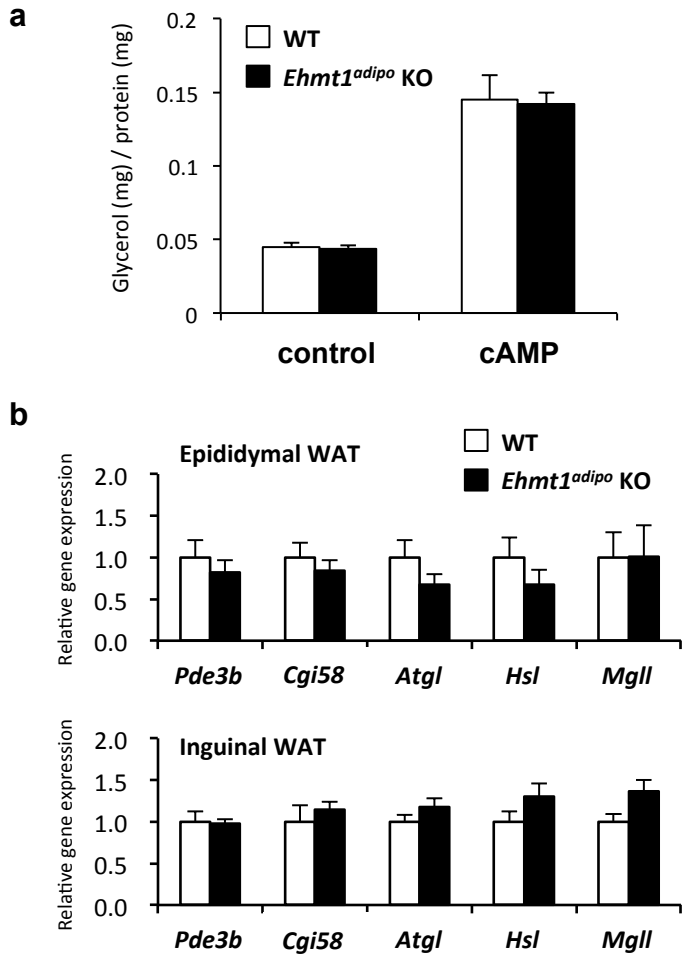

Supplementary Figure 18. Lipolysis capacity in WAT from *Ehmt1*^{adipo} KO mice was indistinguishable from wild-type mice.

a, Glycerol release was measured in primary adipocytes isolated from the epididymal WAT of wild-type and *Ehmt1*^{adipo} KO mice. The adipocytes were treated with or without cAMP (isoproterenol, 1 μM) for 1.5 hours. n=3. **b,** mRNA levels of genes involved in fat lipolysis (as indicated) were measured in the epididymal WAT (upper panel) and in the inguinal WAT (lower panel) by qRT-PCR. n=3-5 per group; data are presented as mean and s.e.m. Note that no statistical difference was found between wild-type and *Ehmt1*^{adipo} KO mice.

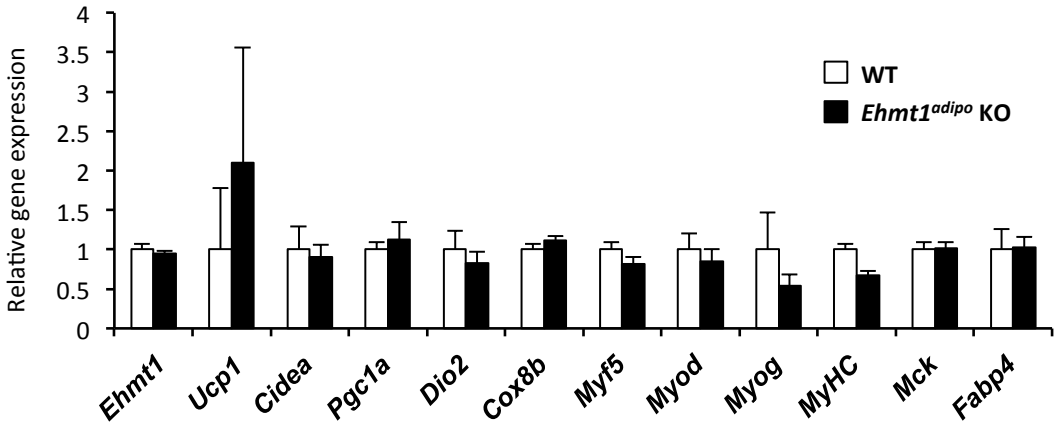

Supplementary Figure 19. Expression of BAT- and skeletal muscle-selective genes were not altered in the skeletal muscle of *Ehmt1*^{adipo} KO mice in response to cold exposure.

Total RNA was extracted from the skeletal muscle of wild-type and *Ehmt1*^{adipo} KO mice after cold exposure (4˚C) for 5 hours. mRNA levels of genes (as indicated) were measured by qRT-PCR. n=6 per group; data are presented as mean and s.e.m.

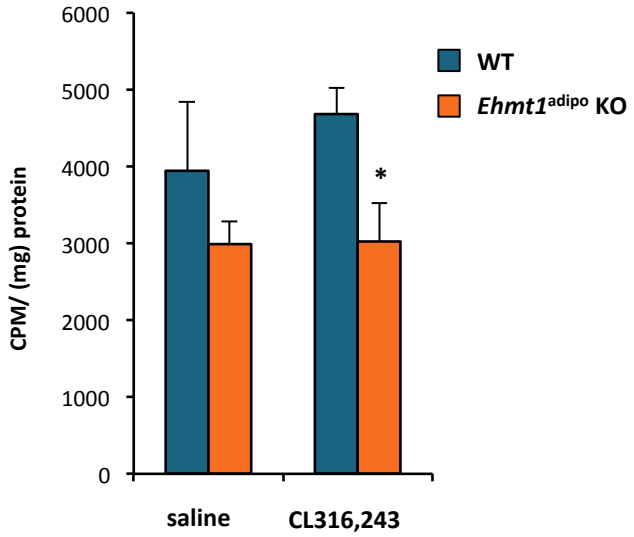

Supplementary Figure 20. Fatty acid uptake was reduced in the BAT of *Ehmt1*^{adipo} KO mice.

Wild-type and *Ehmt1*^{adipo} KO mice were injected intraperitoneally with saline or CL316,243 at a dose of 0.5 mg/kg. Six hours after the injection, BAT were isolated and incubated in DMEM containing ^{14}C-Oleic acid for 15min. ^{14}C radioactivity in the BAT was measured by liquid scintillation counter and normalized to the total protein content. n=4; data are presented as mean and s.e.m.; * $P< 0.05$.

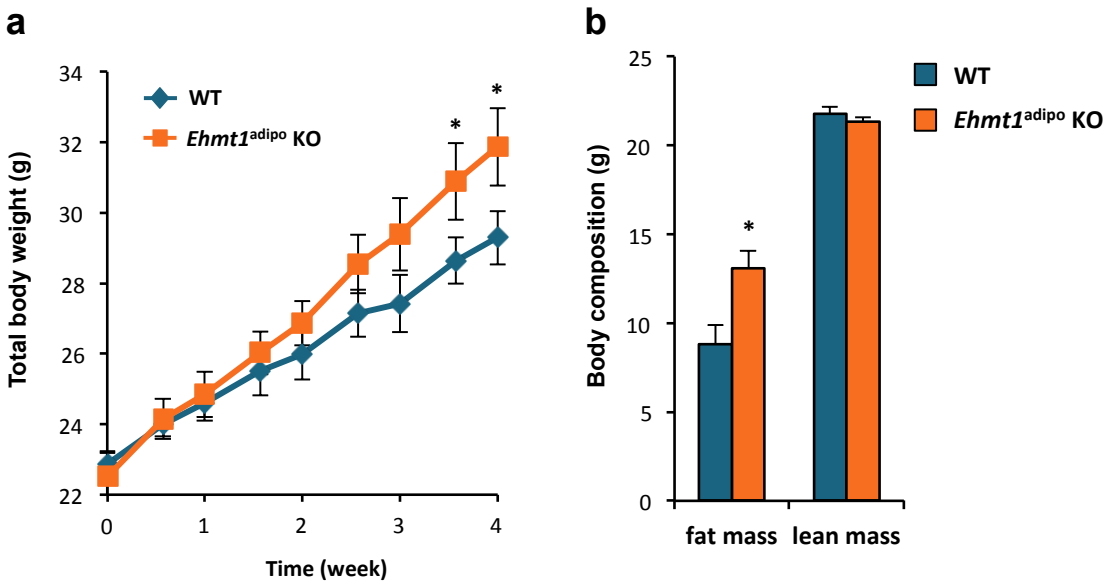

Supplementary Figure 21. Total body weight and body composition of wild-type and *Ehmt1*^{adipo} KO mice under a high-fat diet.

a, Male mice at 6-week-old were kept in individual cages under a high-fat diet at thermoneutrality. Total body weight of each mouse was monitored for 4 weeks. n=16. Genotype and time interaction effect was statistically significant. (P = 0.0113) **b,** Body composition (fat and lean mass) in wild-type and *Ehmt1*^{adipo} KO mice after 4 weeks of high fat diet, as assessed by Magnetic resonance imaging system (EchoMRI-3in1, Echo Medical Systems). Data are presented as mean and s.e.m.; * P< 0.05.

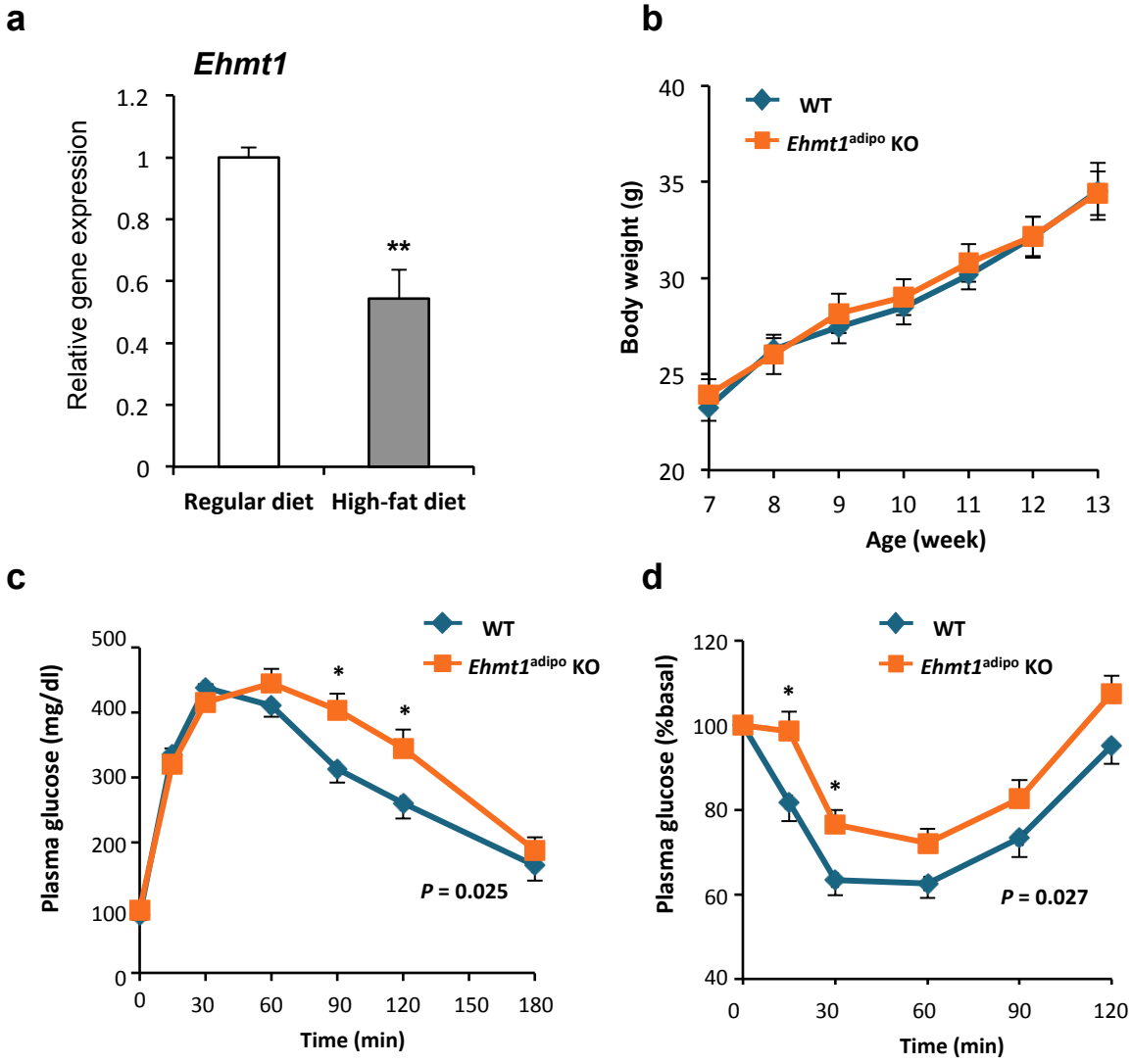

Supplementary Figure 22. Metabolic phenotypes of *Ehmt1*^{adipo} KO mice under a high-fat diet at ambient temperature.

a, mRNA expression of *Ehmt1* was measured by qRT-PCR in the interscapular BAT from wild-type mice under a regular diet or high-fat diet for 14 weeks. n=4. **b,** Body weight increase of wild-type (WT) and *Ehmt1*^{adipo} KO mice under a high-fat diet at ambient temperature. **c,** Glucose tolerance test in 9-week high-fat diet-fed wild-type (WT) and *Ehmt1*^{adipo} KO mice. Serum glucose levels were measured after an overnight fast (time 0) and at the indicated times after an intraperitoneal injection of glucose. The genotype and time interaction was significant (P<0.05). **h,** Insulin tolerance test in 10-week high-fat diet-fed wild-type (WT) and *Ehmt1*^{adipo} KO mice. Serum glucose levels were after an overnight fast (time 0) and at the indicated times after an intraperitoneal injection of insulin (0.75U/kg). n=8-12 per genotype. Data are presented as mean and s.e.m.; * P< 0.05, ** P <0.01.

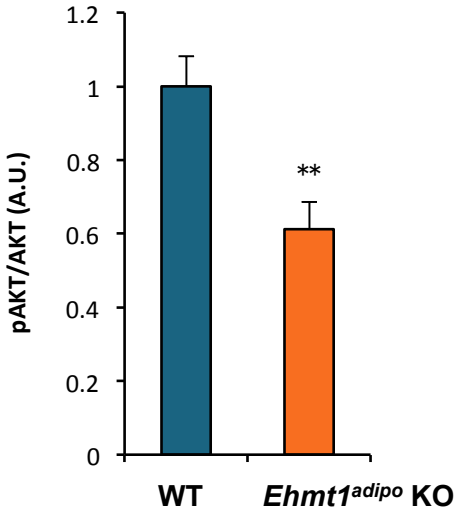

Supplementary Figure 23. Impaired insulin signaling in the liver of *Ehmt1*^{adipo} KO mice under a high-fat diet.

Insulin (5U) was injected into the inferior venae cavae of wild-type and *Ehmt1*^{adipo} mice. Two minutes after the injection, liver tissues were lysed. Phosphorylated (S473) and total Akt proteins were detected by Western blotting. The bands were quantified by Image J software. n=5 per genotype. Data are presented as mean and s.e.m.; ** P <0.01.

Table S1. Metabolic parameters of WT and *Ehmt1*^{adipo} KO mice at thermoneutrality.

Food intake (n=6)	**WT**	***Ehmt1*^{adipo}KO**	***P* value**
Food intake (day, g/12h)	0.9±0.1	1.0±0.1	*P* = 0.47
Food intake (night, g/12h)	1.8±0.1	1.7±0.1	*P* = 0.66

Serum (n=8)	**WT**	***Ehmt1*^{adipo}KO**	***P* value**
Insulin [mg/dl]	1.21±0.13	1.84±0.22 *	*P* < 0.05
Triglycerides [mg/dl]	78±3	72±6	*P* = 0.39
Free fatty acid [mmol/l]	0.61±0.03	0.61±0.06	*P* = 0.91

Weight (n=16)	**WT**	***Ehmt1*^{adipo}KO**	***P* value**
Body weight (g)	29.3±0.8	31.9±1.1 *	*P* < 0.05
Liver (g)	1.11±0.03	1.16±0.04	*P* = 0.39
Heart (g)	0.121±0.002	0.128±0.007	*P* = 0.47

Supplementary Table 2. Primer sequences

Gene	Usage	Forward Primer	Reverse Primer
Acts	qPCR	CCCAAAGCTAACCGGGAGAAG	CCAGAATCCAACACGATGCC
Adipoq	qPCR	GCACTGGCAAGTTCTACTGCAA	GTAGGTGAAGAGAACGGCCTTGT
Atgl	qPCR	CCAACGCCACTCACATCTAC	CCTCAATAATGTTGGCACCTG
Cd137	qPCR	CGTGCAGAACTCCTGTGATAAC	GTCCACCTATGCTGGAGAAGG
Cgi58	qPCR	TGGTGTCCCACATCTACATCA	CAGCGTCCATATTCTGTTTCCA
Cidea	qPCR	ATCACAACTGGCCTGGTTACG	TACTACCCGGTGTCCATTTCT
Cited1	qPCR	AACCTTGGAGTGAAGGATCGC	GTAGGAGAGCCTATTGGAGATGT
Cox3a	qPCR	GCAGGATTCTTCTGAGCGTTCT	GTCAGCAGCCTCCTAGATCATGT
Cox5b	qPCR	GCTGCATCTGTGAAGAGGACAAC	CAGCTTGTAATGGGTTCCACAGT
Cox7a	qPCR	CAGCGTCATGGTCAGTCTGT	AGAAAACCGTGTGGCAGAGA
Cox8b	qPCR	GAACCATGAAGCCAACGACT	GCGAAGTTCACAGTGGTTCC
Cryab	qPCR	GTTCTTCGGAGAGCACCTGTT	GAGAGTCCGGTGTCAATCCAG
Dio2	qPCR	CAGTGTGGTGCACGTCTCCAATC	TGAACCAAAGTTGACCACCAG
Ehmt1	qPCR	GGCACCTTTGTCTGCGAATAC	AGAACCGAGCGTCAATGCAG
Elovl3	qPCR	TCCGCGTTCTCATGTAGGTCT	GGACCTGATGCAACCCTATGA
Fabp4	qPCR	ACACCGAGATTTCCTTCAAACTG	CCATCTAGGGTTATGATGCTCTTCA
Flnc	qPCR	GAAGGCCAACATCCGAGACAA	AGGGCGAGTAAGGGATCTCAT
Hsl	qPCR	CACACCTACTACACAAATCC	GGCATAGTAGGCCATAGCA
Mck	qPCR	GCAAGCACCCCAAGTTTGA	ACCTGTGCCGCGCTTCT
Mgll	qPCR	ACTCTGACCCACTCGTCTGC	CAGCAGGAATGGCAGTGTC
Mhc	qPCR	TCCAAACCGTCTCTGCACTGTT	AGCGTACAAAGTGTGGGTGTGT
Myf5	qPCR	CAGCCCCACCTCCAACTG	GGGACCAGACAGGGCTGTTA
Myl6b	qPCR	AAGCCTGCTGCCAAGTCTAC	ATCACCACTTTGGAGAGATCAAC
Mylpf	qPCR	TTCAAGGAGGCGTTCACTGTA	TAGCGTCGAGTTCCTCATTCT
Myod	qPCR	CGCCACTCCGGGACATAG	GAAGTCGTCTGCTGTCTCAAAGG
Myogenin	qPCR	CCTTAAAGCAGAGAGCATCC	GGAATTCGAGGCATATTATGA
Pde3b	qPCR	TCCTGAACATCTTGCCACTG	AGTACCGCGGAGGAAAAAGT
Pdli3	qPCR	TGGGGGCATAGACTTCAATCA	CTCCGTACCAAAGCCATCAATAG
Pgc1α	qPCR	AGCCGTGACCACTGACAACGAG	GCTGCATGGTTCTGAGTGCTAAG
PparY2	qPCR	GCATGGTGCCTTCGCTGA	TGGCATCTCTGAGTCAACCATG
Prdm16	qPCR	GGCGAGGAAGCTAGCCAAA	GGTCTCCTCCTCGGCACTCT
Ryr1	qPCR	CAGTTTTTGCGGACGGATGAT	CACCGGCCTCCACAGTATTG
Tbp	qPCR	ACCCTTCACCAATGACTCCTATG	TGACTGCAGCAAATCGCTTGG
Tnni1	qPCR	ATGCCGGAAGTTGAGAGGAAA	TCCGAGAGGTAACGCACCTT
Tpm2	qPCR	GTGGCTGAGAGTAAATGTGGG	TTGGTGGAATACTTGTCCGCT
Ucp1	qPCR	CACCTTCCCGCTGGACACT	CCCTAGGACACCTTTATACCTAATGG
Acts	ChIP qPCR	CCTGGACACACGATTGCTGAC	TTTCCATCCCTACCTGGAGC
Gapdh	ChIP qPCR	AAGCCAAACTAGCAGCTAGG	GGGCTAGTCTATCATTGCAG
Mylpf	ChIP qPCR	TCTTCCAGAACTGTGGGCTTCC	GGATGCAAGTCTCGTTAGGACC
Myogenin	ChIP qPCR	GAATCACATGTAATCCACTGGA	ACACCAACTGCTGGGTGCCA
Ryr1	ChIP qPCR	ACCTGTTGTCCCAAGTCCCATC	CCTTGGCTTCAGCCTTCTGC
Tnni1	ChIP qPCR	AGGGTCTCTGTTTGCTGACTG	AGGCTTCAGGAGGTAGACAG